

## Article

# Analyzing Spatial-Temporal Change of Vegetation Ecological Quality and Its Influencing Factors in Anhui Province, Eastern China Using Multiscale Geographically Weighted Regression

Tao Wang<sup>1,2,3</sup>, Mingsong Zhao<sup>1,2,3,\*</sup>, Yingfeng Gao<sup>1,2,3</sup>, Zhilin Yu<sup>1,2,3</sup> and Zhidong Zhao<sup>1,2,3</sup><sup>1</sup> School of Geomatics, Anhui University of Science and Technology, Huainan 232001, China<sup>2</sup> Key Laboratory of Aviation-Aerospace-Ground Cooperative Monitoring and Early Warning of Coal Mining-induced Disasters of Anhui Higher Education Institutes, Anhui Provincial Department of Education, Huainan 232001, China<sup>3</sup> Coal Industry Engineering Research Center of Collaborative Monitoring of Mining Area's Environment and Disasters, Huainan 232001, China

\* Correspondence: zhaomingsonggis@163.com

**Abstract:** Vegetation is a crucial component of terrestrial ecology and plays a significant role in carbon sequestration. Monitoring changes in vegetation ecological quality has important guidance value for sustainable development. In this study, we investigated the spatial and temporal variation characteristics of Ecological Quality Index of Terrestrial Vegetation (EQI) in Anhui Province during the growing season from 2000 to 2020 using trend analysis, partial correlation analysis and bivariate spatial autocorrelation analysis. Based on the Multiscale Geographically Weighted Regression (MGWR), the spatial heterogeneity of the effects of average temperature, precipitation, elevation, slope, and human activity factors on EQI was explored. Our results showed an increasing trend in EQI during the growing season in Anhui Province from 2000 to 2020. The significantly increasing areas accounted for 43.49%, while the significantly decreasing areas accounted for 3.60%. EQI had a mostly positive correlation with precipitation and a negative correlation with average temperature ( $p < 0.1$ ), showing a higher sensitivity to precipitation than to temperature. Additionally, EQI tended to increase initially and then decrease with increasing elevation and slope. Furthermore, our analysis revealed a significant negative spatial correlation between human activity intensity and EQI ( $p < 0.01$ ). The bivariate global autocorrelation Moran index between EQI and human activity in 2000, 2005, 2010, 2015, and 2018 were  $-0.418$ ,  $-0.427$ ,  $-0.414$ ,  $-0.487$ , and  $-0.470$ , respectively. We also found that the influencing factors explain 63–83% of the spatial variation of EQI, and the order of influence of factors on EQI is elevation > human activity > slope > average temperature > precipitation. MGWR results indicated that human activities and topographic factors had a stronger impact on EQI at the local scale, while climate factors tended to influence EQI at the global scale.



**Citation:** Wang, T.; Zhao, M.; Gao, Y.; Yu, Z.; Zhao, Z. Analyzing Spatial-Temporal Change of Vegetation Ecological Quality and Its Influencing Factors in Anhui Province, Eastern China Using Multiscale Geographically Weighted Regression. *Appl. Sci.* **2023**, *13*, 6359. <https://doi.org/10.3390/app13116359>

Academic Editor: Nathan J. Moore

Received: 11 April 2023

Revised: 18 May 2023

Accepted: 22 May 2023

Published: 23 May 2023

**Keywords:** vegetation ecological quality; spatial and temporal variation; Google Earth Engine; human activities; bivariate spatial autocorrelation; multiscale geographic weighted regression



**Copyright:** © 2023 by the authors. Licensee MDPI, Basel, Switzerland. This article is an open access article distributed under the terms and conditions of the Creative Commons Attribution (CC BY) license (<https://creativecommons.org/licenses/by/4.0/>).

## 1. Introduction

Vegetation plays a vital role in the terrestrial ecosystem, serving as a significant carbon sink and a green indicator of terrestrial ecology quality, with obvious interannual change characteristics [1–3]. Therefore, the study of vegetation change is an important part of the assessment of regional ecology. Recently, scientists have mostly used Normalized Difference Vegetation Index (NDVI), Net Primary Productivity (NPP) or Fractional Vegetation Cover (FVC) as a single vegetation index to study spatial and temporal vegetation changes [4–6]. With the development of remote sensing cloud computing platform, which breaks the limitation of local storage, large scale and long time series research on monitoring vegetation change has gained a significant momentum [7,8]. Google Earth Engine (GEE) is a remote

sensing data processing cloud platform launched by Google in 2000 to enable online visualization, computation and analysis of large, long time series and multi-scale Earth data (mainly satellite data) [9]. Compared to traditional desktop remote sensing processing platforms (such as ENVI and ERDAS software), GEE has two major advantages: (1) it provides online access to satellite remote sensing data from different sources and scales, and users can also upload their own data, breaking the limitation of local data storage; and (2) it provides a variety of algorithms and API interfaces, such as cloud masking and radiation correction, which allow users to process remote sensing images flexibly and autonomously [10]. This has led to an increasing number of studies based on the GEE platform in recent years [11]. Taking advantage of the convenience provided by the GEE platform, this study integrates the primary data acquisition and processing steps into the platform.

Temperature and precipitation are the main climatic factors affecting vegetation growth [12], but the effects of topographic factors and human activities on vegetation growth should not be neglected. Most previous studies have directly and quantitatively assessed the relationship between vegetation indices and climate or topography [6,13], and fewer studies have assessed the impact of human activities on vegetation ecology. Some characterize human activities with a single data, such as Zhou et al. [14], who used crop yield and afforestation to explain the ecological disturbance caused by human activities, and Luo et al. [15], who used population data as a proxy for human activities. Some studies quantified the residuals after excluding the ecological effects of natural factors, such as the effects of human activities on vegetation and climate, and some other studies, such as Cheng et al. [16], Luo et al. [17] and Zhang et al. [18], used residual analysis to indirectly derive the effects of human activities, none of which can quantify human activities. The concept of human footprint was introduced by Sanderson et al. [19] in 2002 to reflect the impact of human activities on ecosystems, climate and human health [20]. Existing free global human footprint datasets are mapped based on eight categories of variables: built environment, population density, electrical infrastructure, agricultural land, grazing land, roads, railways and navigable waterways [21,22]. In this paper, we introduce the Human Footprint dataset to quantitatively study the impact of human activities on vegetation ecological quality. The influence of climate, topography and human activities on vegetation ecology has obvious regional characteristics. The classical Geographically Weighted Regression (GWR) model can reflect this pattern at one scale (same bandwidth), but it ignores the effect of drivers at different scales. Multiscale Geographically Weighted Regression (MGWR) can quantitatively assess the spatial variability of the effects of drivers at different scales. Based on this characteristic, MGWR has been applied in several areas, such as exploring the spatial heterogeneity of PM<sub>2.5</sub> forcing factors [23,24], modeling urban ozone drivers [25], and integrating nighttime lighting with multi-source urban data [26]. However, it has not yet been applied to explore the driving factors of vegetation ecological quality. Therefore, we use MGWR to construct a spatial impact model of climate, topography, and human activity factors on EQI.

During the 14th Five-Year Plan period, Anhui Province is firmly promoting the construction of ecological civilization. As the primary producer of the ecosystem, the evaluation of vegetation quality can be regarded as the core content of ecological quality assessment. In this study, the Ecological Quality Index of Terrestrial Vegetation (EQI) calculated via NPP and FVC was used to reflect the vegetation function and cover status of terrestrial ecosystems in Anhui Province during the growing season (April–October) [27]. Using the GEE platform, the time series of EQI in Anhui Province for the past 20 years were constructed to analyze the spatial and temporal variation characteristics of EQI. Partial correlation analysis, spatial bivariate autocorrelation and MGWR were used to quantitatively evaluate the spatial variability of the effects of natural and anthropogenic activities on EQI. This study aims to provide scientific and reasonable information on the construction of ecological civilization in Anhui Province in terms of climate, topography and human activities.

## 2. Study Area and Data

### 2.1. Study Area

Anhui Province, located in eastern China, has coordinates of  $114^{\circ}54' \sim 119^{\circ}37'$  E and  $29^{\circ}41' \sim 34^{\circ}38'$  N, covering a total area of  $1.4 \times 10^5$  km<sup>2</sup>. The province belongs to the transition area between the warm temperate zone and subtropical zone, characterized by an average temperature of 14–18 °C and annual precipitation of 800–1800 mm. With elevations ranging from 0 to 1743 m, Anhui Province's topography exhibits a “high in the south and low in the north” pattern (Figure 1). The southern and Dabie Mountains are mountainous areas dominated by woodlands, while the Huabei Plain and Jianghuai Hills serve as centers for human activities.

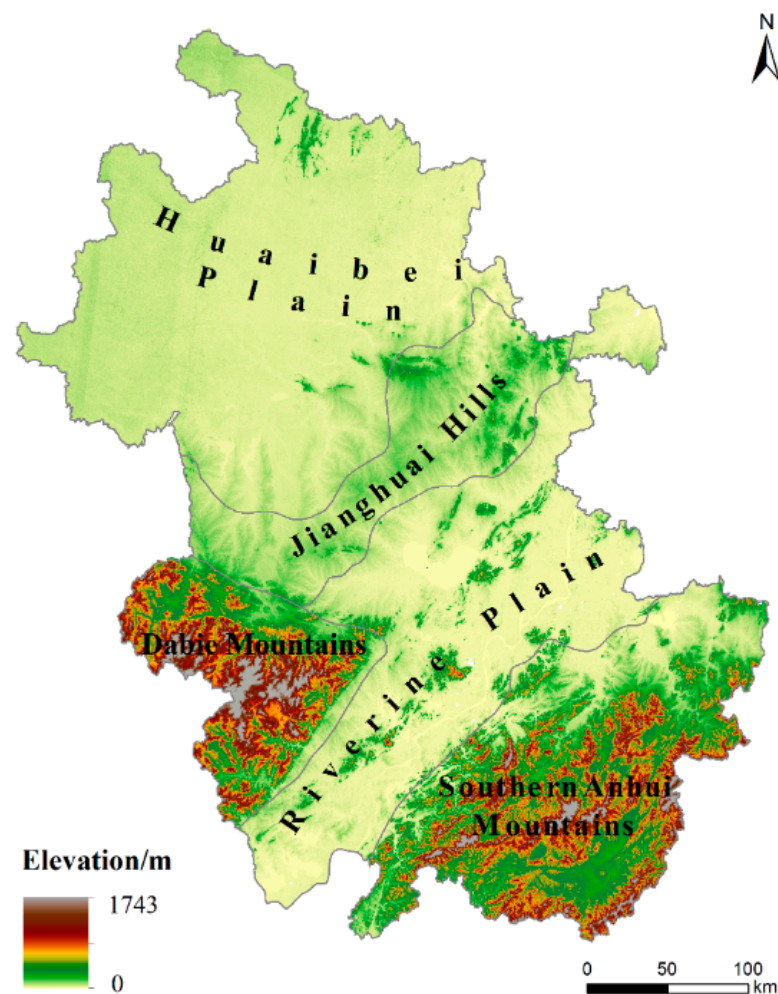


**Figure 1.** Topographic map of Anhui Province.

### 2.2. Data Source

Spatial data include MODIS data products (NDVI, and NPP), meteorological data (precipitation, and average temperature), DEM, and human footprint (Table 1). MODIS product data, meteorological data and DEM can be called directly in GEE. The human footprint is taken from the dataset shared by Mu et al. [21] and refer to human activities in the paper.

**Table 1.** Data sources.

Data	Spatial Resolution	Time Resolution	Website/GEE Dataset
NDVI	500 m	1 year	MODIS/061/MOD13A
NPP	500 m	8 day	MODIS/006/MOD17A3HG
precipitation	5566 m	1 day	UCSB-CHG/CHIRPS/DAILY
Average temperature	11,132 m	1 month	ECMWF/ERA5_LAND/MONTHLY
DEM	30 m	N/A	projects/sat-io/open-datasets/ASTER/GDEM
Human Footprint	1000 m	1 year	<a href="https://doi.org/10.6084/m9.figshare.16571064">https://doi.org/10.6084/m9.figshare.16571064</a> accessed on 15 December 2022.

### 3. Research Methodology

#### 3.1. Data Processing and Analysis

In this study, we conducted a research on multiple platforms (Figure 2). The steps are as follows: (1) On the GEE platform, NDVI and NPP image data of the growing season (April–October) in Anhui Province from 2000 to 2020 are screened for cloud filtering, water masking, and cropping. Then, the FVC is calculated using the dimidiate pixel model, and the EQI of the study area for the corresponding time period is calculated based on the FVC and NPP. (2) In ArcGIS 10.6, trend analysis is used to study the spatial and temporal changes of EQI in Anhui Province from 2000 to 2020, and the distribution characteristics of EQI at different elevations and slopes are counted using the raster statistics function. (3) To study the effect of average temperature and precipitation on EQI partial correlation analysis is implemented in R. (4) Then the spatial correlation between human activities and EQI with bivariate Moran index is studied using the GeoDa software. (5) In MGWR2.2.1, spatial regression models between climate, topography, human activity factors and EQI are developed to analyze the spatial heterogeneity of their EQI influencing factors.

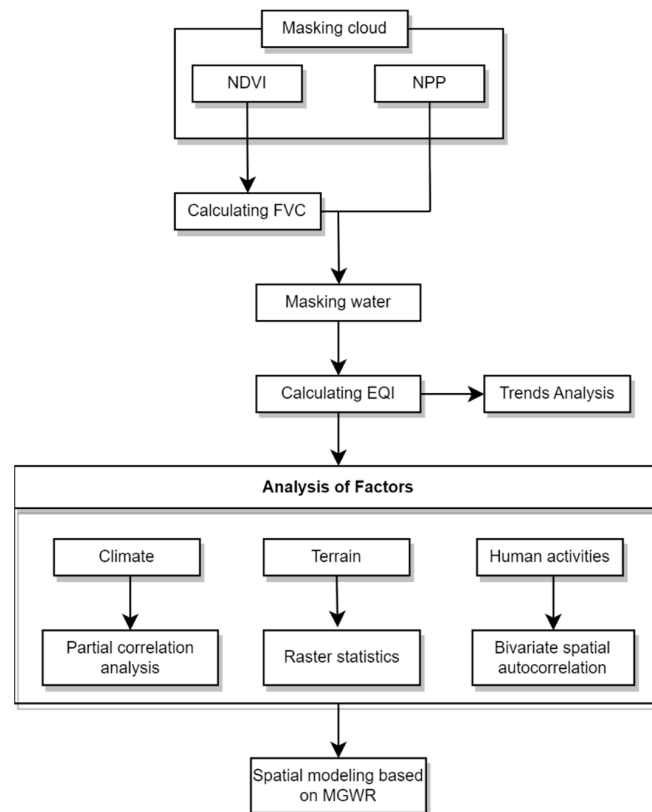


**Figure 2.** Flow chart of data processing.

### 3.2. Ecological Quality Index of Terrestrial Vegetation

The Ecological Quality Index of Terrestrial Vegetation is a quantitative value based on the weighted net productivity and cover of vegetation, and its magnitude reflects the high or low ecological quality of vegetation:

$$EQI = \left( FVC \times f_1 + \frac{NPP}{NPP_{max}} \times f_2 \right) \times 100 \tag{1}$$

where, EQI is the ecological quality index of vegetation in the growing season, varying from 0 to 100;  $f_1$  is the weighting factor of vegetation cover, taking 0.5; FVC is the vegetation cover in the period;  $f_2$  is the weighting factor of net primary productivity of vegetation, taking 0.5; NPP is the cumulative net primary productivity of vegetation in the period; and  $NPP_{max}$  is the maximum of net primary productivity of terrestrial vegetation in the same period of the calendar year, i.e., the best NPP is the net primary productivity of vegetation under the best meteorological conditions. According to QX/T 494-2019 [27], the ecological quality index of land vegetation in Anhui Province was classified into five classes, where  $Q < 20$  was very poor,  $20 \leq Q < 40$  was poor,  $40 \leq Q < 60$  was moderate,  $60 \leq Q < 80$  was good, and  $80 \leq Q < 100$  was excellent.

### 3.3. Trend Analysis

Based on the ArcGIS 10.6 plugin Curve Fit [28], a one-dimensional linear fit of EQI from 2000 to 2020 was performed to obtain the slope and  $p$ -value to examine the spatial distributional properties of EQI changes:

$$b_{Slope} = \frac{n \times \sum_{i=1}^n (i \times EQI_i) - \sum_{i=1}^n i \times \sum_{i=1}^n EQI_i}{n \times \sum_{i=1}^n i^2 - (\sum_{i=1}^n i)^2} \tag{2}$$

where,  $b_{Slope}$  is the slope of the EQI linear regression;  $n$  is the total number of years and in this study  $n = 21$  was taken;  $i$  is the year; and  $EQI_i$  is the EQI value of year  $i$ . The obtained EQI slopes and  $p$ -values were analyzed overlaid and divided into five classes: highly significant decrease ( $b < 0, p < 0.01$ ), significant decrease ( $b < 0, p < 0.05$ ), significant increase ( $b > 0, p < 0.05$ ), highly significant increase ( $b > 0, p < 0.01$ ) and insignificant ( $p > 0.05$ ).

### 3.4. Partial Correlation Analysis

Partial correlation analysis has been widely used to study the relationship between vegetation and climate factors, examining the relationship of a single climate factor while excluding the influence of other climate factors [29,30]. In this article, we examine the partial correlation between EQI and temperature and precipitation based on the terra and ppcor packages in R language. The calculation equation is as follows:

$$r_{xy,z} = \frac{r_{xy} - r_{xz}r_{yz}}{\sqrt{(1 - r_{xz}^2)(1 - r_{yz}^2)}} \tag{3}$$

where,  $x$  is the EQI;  $y$  is average Temperature and  $z$  is precipitation; and  $r_{xy,z}$  is the partial correlation coefficient between temperature and EQI after precipitation fixation.

### 3.5. Bivariate Spatial Autocorrelation Analysis

Spatial autocorrelation is divided into global autocorrelation and local autocorrelation, and the most commonly used statistic is Moran’s index (Moran’s I). The global Moran’s I mainly describes the average degree of global correlation of spatial units with their neighbors, while the local Moran’s I reflects the spatial aggregation of correlations [31–33]. In this paper, the spatial relationship between human activities and EQI in Anhui Province

from 2000 to 2018 is investigated using the “bivariate Moran’s I” function of GeoDa software, in which the bivariate local Moran’s I index is formulated as follows.

$$I_{kl}^i = z_k^i \sum_{j=1}^n w_{ij} z_l^j \quad (4)$$

$$z_k^i = \frac{x_k^i - \bar{x}_k}{\sigma_k}, z_l^i = \frac{x_l^i - \bar{x}_l}{\sigma_l} \quad (5)$$

where,  $I_{kl}^i$  is the Moran index of variable  $k$  and variable  $l$  at  $i$ ;  $w_{ij}$  is the spatial weight matrix between  $i$  and  $j$ ;  $\bar{x}_k$  is the mean of variable  $k$ ;  $x_k^i$  is the value of variable  $k$  at  $i$ ; and  $\sigma_k$  is the variance of variable  $k$  [34,35]. To reduce data magnitude and improve the efficiency of software execution, the raster images were uniformly resampled to 5 km in ArcGIS 10.6 software, and then the raster transfer points were executed to obtain 3574 vector points for evaluation and processing.

### 3.6. Multiscale Geographic Weighted Regression

In MGWR2.2.1, the spatial kernel function selects the Adaptive type, the optimal bandwidth is determined using the AICc criterion, and the variable normalization is checked [36]. The range of each variable in the MGWR model is different and better describes the spatial effect of the influencing factor on the dependent variable heterogeneity [37], and MGWR is calculated as follows:

$$y_i = \sum_{j=1}^k \beta_{bwj}(\mu_i, v_i) x_{ij} + \varepsilon_i \quad (6)$$

where,  $y_i$  is the corresponding variable at location  $(\mu_i, v_i)$ ;  $\beta_{bwj}$  is the bandwidth used for the regression coefficient of variable  $j$ ;  $x_{ij}$  is the value of the variable at  $(\mu_i, v_i)$ , and  $\varepsilon_i$  is the random error term.

## 4. Results

### 4.1. Spatial and Temporal Variation of EQI

During the growing season of 2000–2020, the EQI values in Anhui province ranged from 62.47 to 74.93, with a multi-year average of 71.82 (Figure 3). The results indicate a statistically significant increasing trend with an annual growth rate of 0.61%. The trend of the EQI time series was determined using the Mann–Kendall (MK) test and the sliding  $t$ -test (Figure 4). The MK test revealed two cross-points in the curves of UF and UB in 2004 and 2005, respectively, with a significant confidence interval of 0.05. However, the  $t$ -statistic of EQI in the sliding  $t$ -Test did not exceed the significance level of 0.05. By combining both methods, we determined that EQI has significantly increased. Nevertheless, no mutation point could be observed in the EQI time series. From 2000 to 2020, the EQI values in different geographic regions of Anhui province exhibited different degrees of increase (Figure 5). The Jianghuai hills and Huaibei plain had relatively high annual growth rates of 1.49% and 0.91%, respectively, but their interannual fluctuations were large. The ecological quality of vegetation along the river plain was relatively stable, with EQI values fluctuating between 60.58 and 71.83 and an annual growth rate of 0.45%. The Dabie Mountains and Southern Anhui Mountains, which are mainly forested with high vegetation cover, had higher EQI values than other regions and less volatility, with annual growth rates of 0.55% and 0.01%, respectively. The growing season EQI in Anhui Province differed across elevation and slope zones (Figure 6). EQI generally increased with rising elevations when the elevations were less than 600 m, while it decreased gradually with rising elevations when the elevations were greater than 600 m. EQI also increased with rising slope when the slope was between 0 and 18° but decreased with rising slope when the slope was greater than 18°.

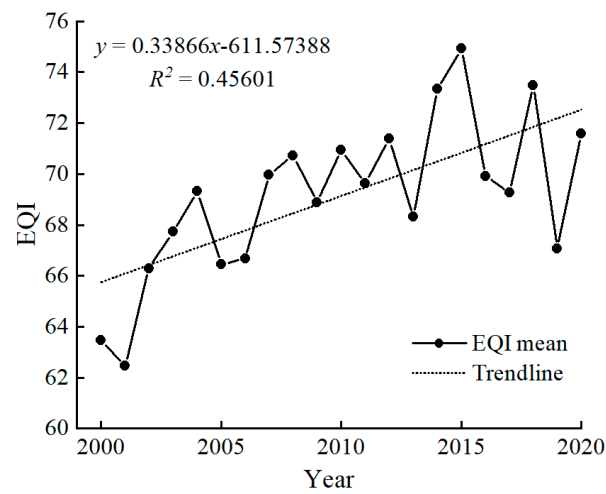


Figure 3. Interannual variation in EQI during the growing season in Anhui Province, 2000–2020.

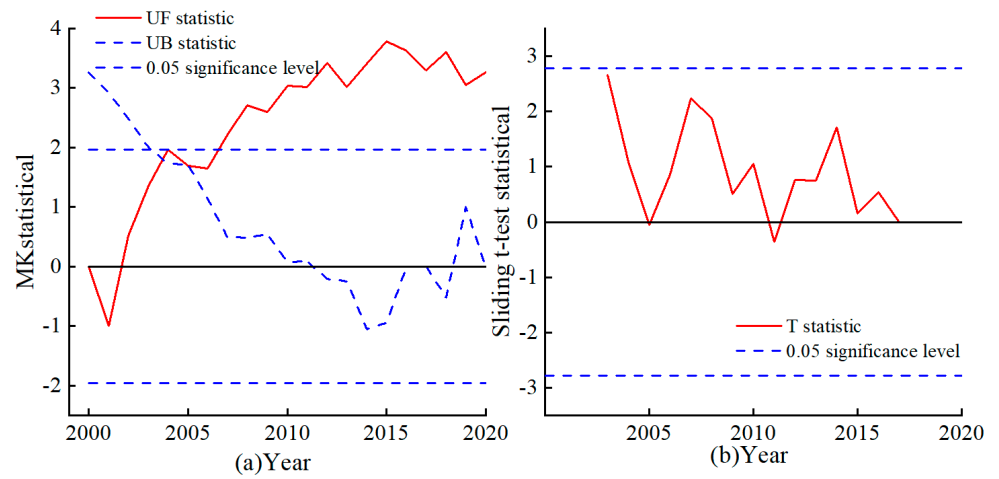


Figure 4. (a) Mann–Kendall test for EQI; (b) Sliding *t*-test for EQI.

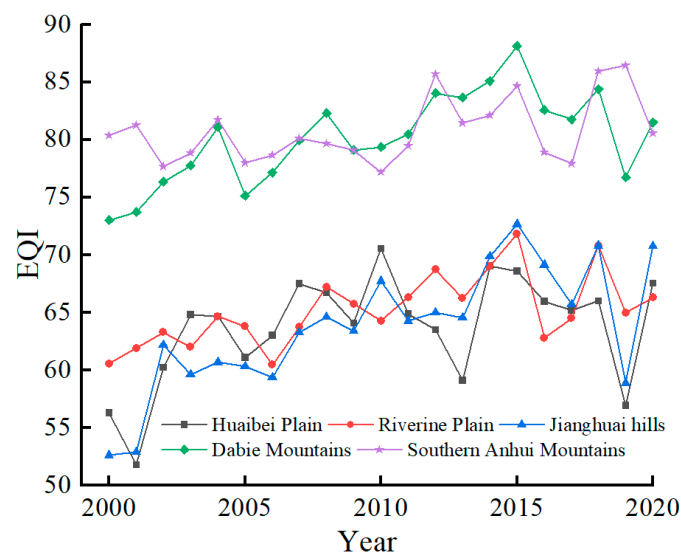
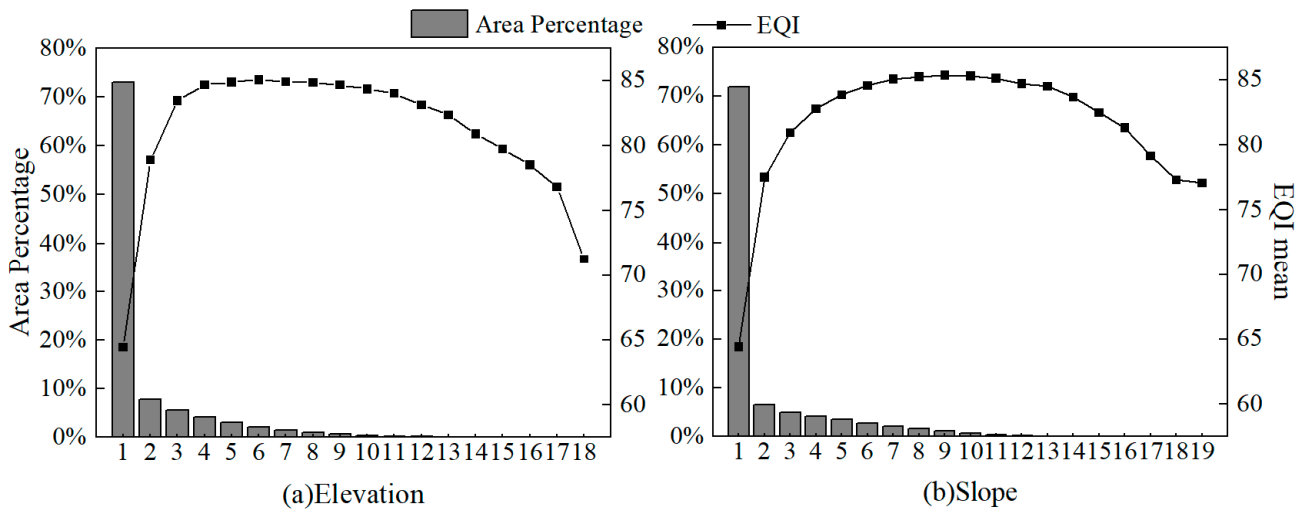
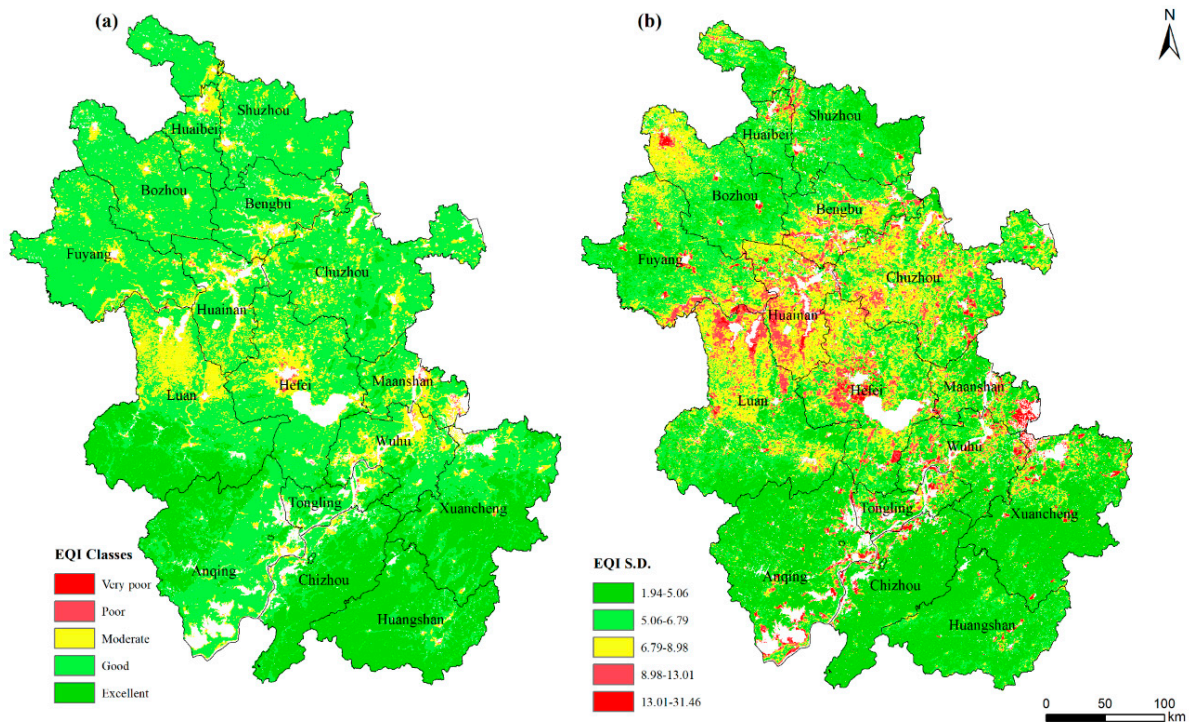


Figure 5. Interannual variation in EQI by geographic region in Anhui Province.



**Figure 6.** Relationship of EQI with elevation (a) and slope (b) in Anhui Province. (a) where 1–19 represent the elevation bands 0–100 m 100–200 m ... 1700–1800 m, respectively, (b) where 1–31 represent slope bands 0–2°, 2–4°, 4–6°, respectively ... 36–38°.

In terms of spatial distribution, the multi-year EQI in Anhui Province has obvious spatial distribution differences (Figure 7a), showing a trend of “good in the south, bad in the north, and the worst in the middle”. The EQI in the Dabie and southern Anhui mountains is the highest, with an average EQI value between 80 and 100 and an EQI grade of “excellent”. EQI in the Huaibei Plain is relatively poor, with EQI grade mostly “good” and “Moderate”. The lowest EQI is distributed in the Hefei city area and the upper Yangtze River basin in the province. Luan, Huainan, Hefei and Maanshan have more fluctuations in EQI over 20 years, while EQI of cities in southern Anhui is more stable (Figure 7b).



**Figure 7.** EQI classes (a) and standard deviations (b) of growing season in Anhui Province, 2000–2020.

From 2000 to 2020, the EQI in most areas of Anhui Province remained basically unchanged, accounting for 52.91%. The area with increase in EQI is much larger than that with decrease. (Figure 8). The regions with very significantly increased and significant increase in EQI account for 30.74% and 12.75% of the land area, respectively, and are mainly located in Huainan, Chuzhou and the northern part of Hefei. The areas with very significantly decreased and significantly decrease in EQI accounted for 2.45% and 1.15%, respectively, and are mainly located in the watershed of the Yangtze River pathway and the central area of Hefei. Active economic development, rapid urban expansion and frequent human activities in these regions are the major factors responsible for the degradation of the ecological quality of the vegetation. Our study found differences in EQI trends across all geographical regions of the province (Table 2). The highest percentage of significant increase in EQI in JiangHuai Hills, accounting for 74.40%, indicates that ecological protection in JiangHuai Hills has been effective in the past 20 years. Riverine Plain, which is the hub of the province's economic centers, has the highest percentage of significantly decreased EQI area, accounting for 8.10%. Dabie Mountains has the least amount of EQI reduction area because of being classified as an ecological reserve. EQI change is least obvious in Southern Anhui Mountains with low footprint of human activities.

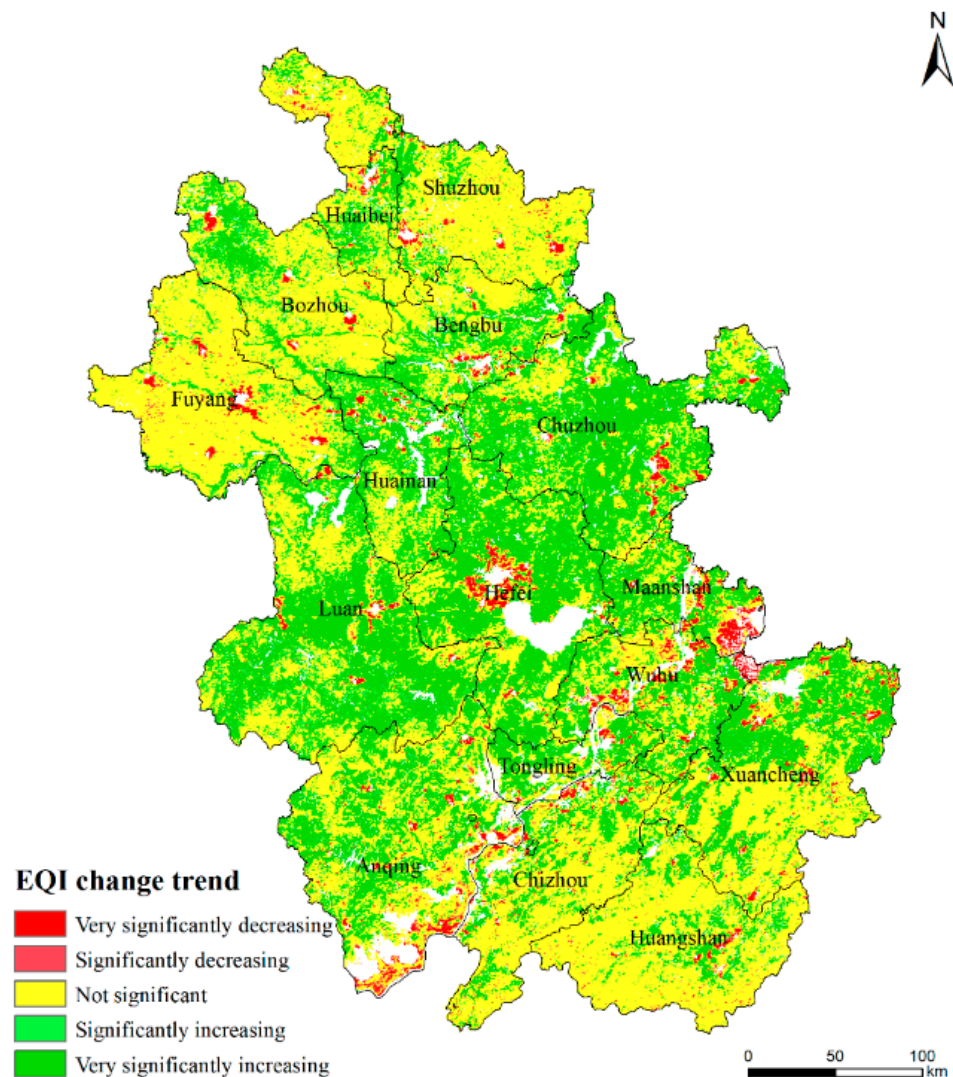


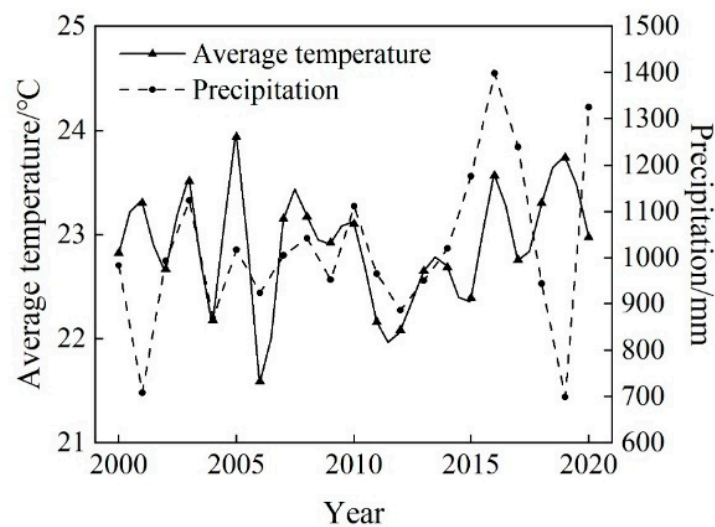
**Figure 8.** Trends of EQI during the growing season in Anhui Province from 2000 to 2020.

**Table 2.** Area ratio of each EQI trend.

Area	Extremely Significant Reduction	Significant Reduction	Not Significant	Significant Increase	Extremely Significant Increase
Huaibei Plain	1.78%	0.95%	63.94%	14.39%	18.95%
Jianghuai hills	1.21%	0.51%	23.88%	13.54%	60.86%
Riverside Plain	5.75%	2.35%	41.50%	11.80%	38.60%
Dabie Mountains	0.73%	0.38%	40.78%	17.45%	40.66%
Southern Anhui Mountains	1.85%	1.02%	65.96%	8.50%	22.67%

#### 4.2. Impact of Temperature and Precipitation on EQI

From 2000 to 2020, the growing season temperature in Anhui Province ranged from 21.58 to 23.93 °C, with a multi-year average of 22.89 °C, showing a slow first decreasing and then an increasing trend. Precipitation ranged from 698.63 to 1398.72 mm, with a multi-year average of 1015.95 mm, fluctuating slowly upward (Figure 9). Spatially, the average temperature decreases from south to north, with the lowest temperature in the Dabie Mountains and the highest temperature in the south of Anqing. The amount of precipitation tends to decrease from the south to the north, and the maximum precipitation is observed in the cities of southern Anhui and Dabie Mountains.

**Figure 9.** Average temperature and precipitation of growing season in Anhui Province, 2000–2020.

The partial correlation coefficient between EQI and average temperature ranged from  $-0.86$  to  $0.73$ , with a predominantly negative correlation (Figure 10a). The regions with significant negative correlation accounted for 10.61% of the province, mainly in the western region and Southern Anhui Mountains. The significant positive correlation was 0.44%, sporadically distributed in the Huaibei Plain and the upper reaches of the Yangtze River. The correlation between EQI and precipitation is strong, with the number of partial correlation coefficient ranging from  $-0.91$  to  $0.85$ , with a predominantly positive correlation (Figure 10b). The significant positive correlation accounted for 28.56% of the province's land area, and the significant negative correlation accounted for only 9.87%, mainly in Southern Anhui Mountains and the Yangtze River basin.

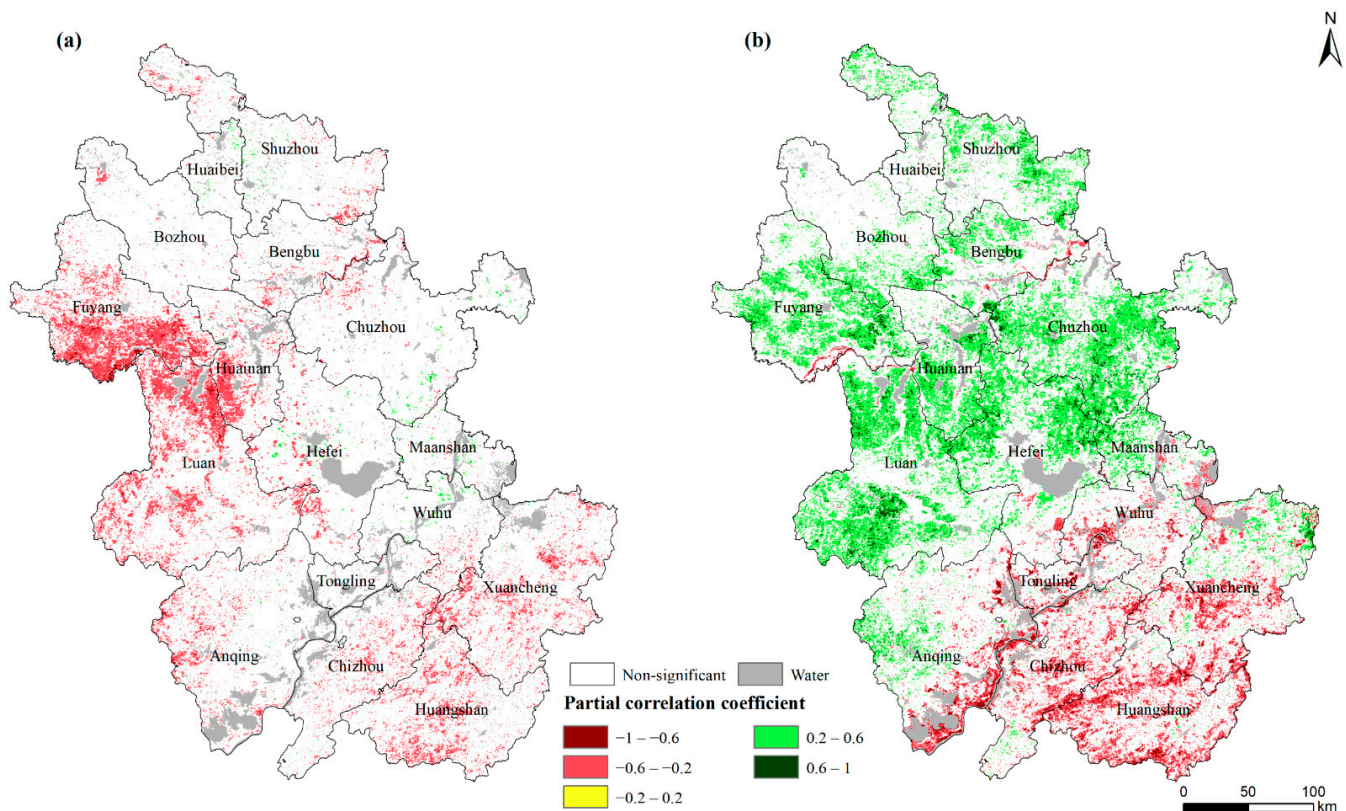


**Figure 10.** Distribution of partial correlation coefficients between EQI and average temperature (a) and precipitation (b) during the growing season in Anhui Province, 2000–2020.

#### 4.3. Spatial Correlation Analysis of Human Activities and EQI

The bivariate global Moran's  $I$  of EQI and human activity for 2000, 2005, 2010, 2015, and 2018 are  $-0.418$ ,  $-0.427$ ,  $-0.414$ ,  $-0.487$ , and  $-0.477$ , respectively ( $p < 0.01$ ). The results indicate that there is a significant negative spatial correlation between human activities and EQI, and that the increase in human activities leads to a decrease in EQI. The spatial dependence between human activity and EQI is dominated by the "high-low", where both high EQI values are surrounded by areas of low human activity (Figure 11). The "high-low" is distributed in the Dabie Mountains and Southern Anhui Mountains, of which the Dabie Mountains is a national key ecological function area to lay the foundation for high EQI. The "low-high" is concentrated in urban centers, where intense human activity, urban sprawl, and low vegetation cover result in low EQI values. The "high-high" is mainly located in the city edge or in the combined suburban areas, where EQI is affected by human transformation and construction, but its vegetation and ecological environment are also strongly protected and maintained under the ecological protection policy.

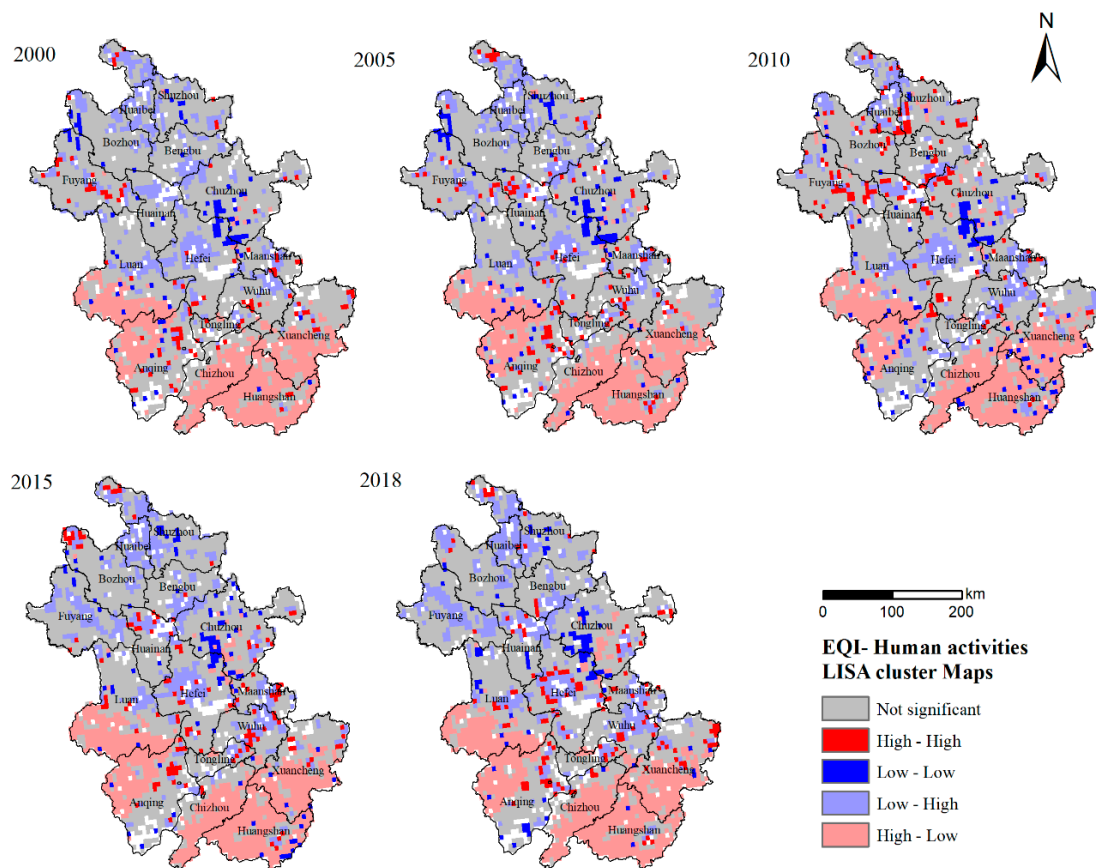


Figure 11. Local spatial clustering of EQI and human activities, 2000–2018.

#### 4.4. Spatial Heterogeneity Analysis of EQI Impact Factors

The different bandwidths of the variables indicate that the variables have different scales of influence. The spatial scales of the effect of the influencing factors on the EQI varied considerably in this study (Table 3). The bandwidths of average temperature and precipitation are significantly larger than those of other variables, illustrating that the scale of action of climate factors on EQI tends to be global and their spatial heterogeneity is weak. The low bandwidth of human activities and elevation showed that human activities and elevation tend to influence EQI at a local scale with high spatial heterogeneity. Factors, such as climate, topography, and human activities explain 63–83% of the spatial variation in EQI, according to the adjusted  $R^2$  of the MGWR model.

Table 3. MGWR model parameters.

Year	MGWR Parameters		Variable Bandwidth				
	AICc	Adj $R^2$	H	T	P	E	S
2000	4215	0.826	217	3573	3573	217	671
2005	5668	0.738	250	314	3573	43	1101
2010	6928	0.633	52	3573	3573	95	706
2015	6376	0.678	121	2388	813	51	1664
2018	5904	0.729	51	3573	3573	1120	325

Where H is human activities; T is average temperature; P is precipitation; E is elevation; and S is slope.

From the MGWR standardized coefficients, the ranking of factors on the EQI was derived as the following: elevation > human activity > slope > average temperature > precipitation (Table 4). Human activities have a negative impact on EQI, and this negative impact increases over time. The average temperature shows an overall negative effect

on the EQI, but the regression coefficient of the average temperature in 2005 shows a divergence, which is due to the fact that the average temperature in Anhui Province in 2005 was the highest in history. Precipitation had a predominantly positive effect on the EQI, with the greatest impact in 2015. Elevation and slope direction have a consistent positive effect on EQI.

**Table 4.** Statistics of standardized regression coefficients of MGWR model.

Year	Regression Coefficient Mean ± Standard Deviation				
	H	T	P	E	S
2000	-0.135 ± 0.594	-0.083 ± 0.003	0.066 ± 0.001	0.323 ± 0.307	0.108 ± 0.104
2005	-0.195 ± 0.128	0.156 ± 0.393	-0.050 ± 0.002	0.34 ± 0.892	0.130 ± 0.074
2010	-0.294 ± 0.224	-0.223 ± 0.002	-0.048 ± 0.006	0.429 ± 0.611	0.091 ± 0.132
2015	-0.327 ± 0.164	-0.136 ± 0.011	0.452 ± 0.401	0.394 ± 0.593	0.135 ± 0.035
2018	-0.237 ± 0.191	-0.108 ± 0.002	0.083 ± 0.007	0.175 ± 0.137	0.388 ± 0.251

The distribution of the MGWR standardized regression coefficients of EQI impact factors is shown in Figure 12. The impact of human activities on EQI was the lowest in the JHH hills and the highest in the city centers. The effect of average temperature on EQI gradually increased from southwest to northeast, and its regression coefficient was negative within the province. Precipitation, with a gradual increase from south to north, had a positive effect on the EQI. The effect of elevation on EQI increases from southwest to northeast. High regression coefficient values are concentrated in Chuzhou. There is a positive spatial correlation between slope and EQI, and the areas with the greatest impact are concentrated in the central eastern part of Anhui Province.

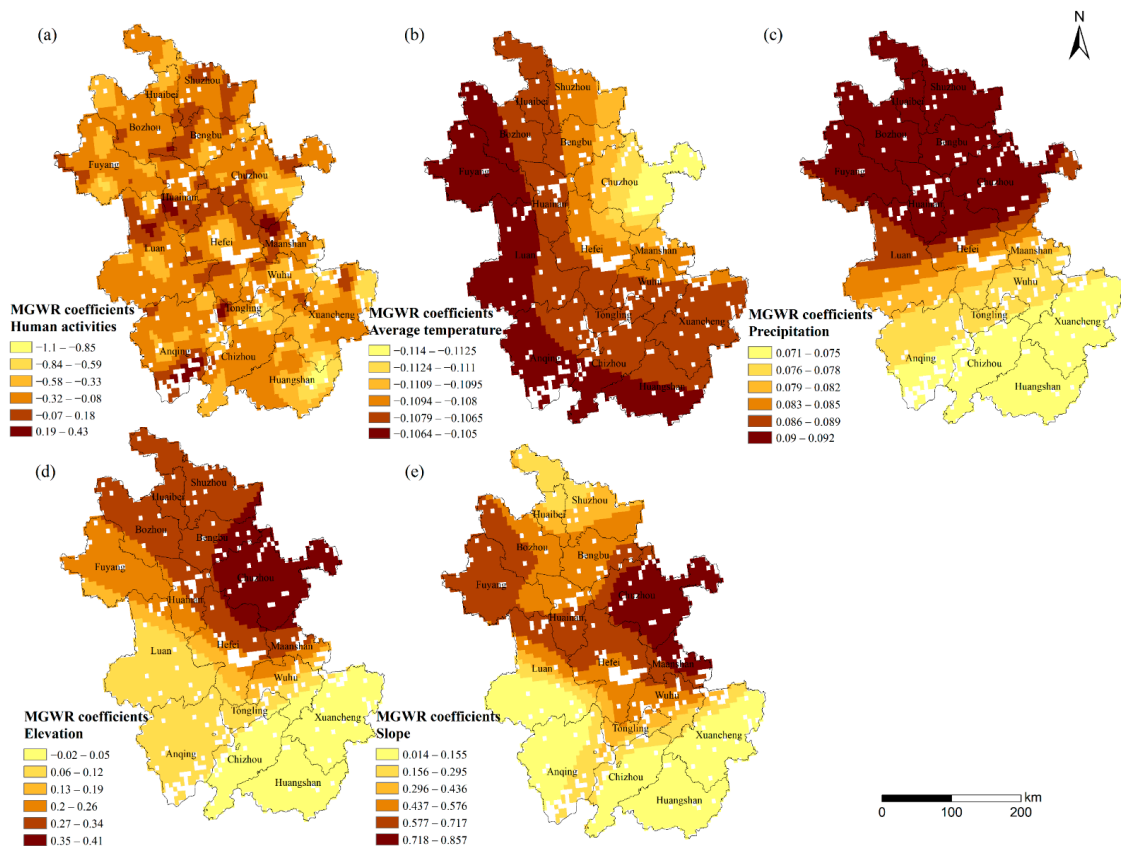


**Figure 12.** Spatial distribution of MGWR regression coefficients for human activity (a), average temperature (b), precipitation (c), elevation (d) and slope (e) in 2018.

## 5. Discussion

The impact of human activities on vegetation growth is a perennial concern among scholars. An objective evaluation of this impact remains elusive, but the residual analysis method has emerged as a popular approach. This method involves fitting and removing natural factors to isolate the impact of human activities [17,18]. For instance, Cheng et al. [16] used this method to quantitatively evaluate the impact of human activities on NDVI in the Qinling Mountains and found that human activities mainly caused vegetation degradation. However, this approach has limitations since it does not account for all natural factors, leading to less accurate assessments of anthropogenic impacts. Another commonly used approach involves representing human activities through single data sets related to human activities, such as nighttime light data and land use data [38,39]. Using nighttime lights, Gu et al. [38] characterized the intensity of human activities and concluded that human activities had a predominantly negative impact on NDVI in Anhui province. However, relying on single data sets may not provide an integrated and comprehensive representation of human activities. On the other hand, mapping human footprint data based on eight human activity variables, including population density, environmental buildings, and land use data, can lead to a more comprehensive quantification of human activities [21]. Human footprint data have been used to evaluate ecological vulnerability on the Tibetan Plateau [40], and explore arable land expansion [41]. In this study, we use human footprint data to directly quantify human activities and accurately assess their impact on vegetation ecology EQI. When assessing the impact of human activities on vegetation ecology, it is important to consider both the positive and negative facets. Figures 11 and 12b in our paper depict the spatial aggregation of human activities and EQI. The “high-high” type is primarily distributed within urban green spaces and nature conservation areas, where anthropogenic afforestation and ecological protection policies have led to a positive impact of human activities on EQI [42,43]. In contrast, the “low-high” type, mainly concentrated in ecologically fragile areas and urban centers, has a negative impact of human activities on EQI. We recommend further strengthening ecological protection and balancing human and ecological needs [44]. Between 2000 and 2018, the “low-high” type proliferated in cities, revealing the ecological challenges arising from social development. It is therefore imperative to accelerate the construction of ecological civilization and maintain a balance between human and ecology.

When studying the drivers of vegetation ecological quality, scholars typically use correlation analysis [45] and principal component analysis [46] to establish mathematical models between vegetation and factors. However, the spatial role of factors' influence on vegetation cannot be ignored, and Geographically Weighted Regression (GWR) models were developed to address this issue. GWR can explain the degree of influence of independent factors on dependent variables at different spatial locations, but this is based on the same scale (same bandwidth). To overcome this limitation, MGWR was developed to allow individual factors to reflect their spatial influence on the target variable at different scales (different bandwidths) [37]. In Li et al.'s study of FVC in Northeast China, temperature affects NDVI at large scales (bandwidth 193) and human activities at small regional scales (bandwidth 27) [47]. Similarly, in Anhui Province, human activities have varying patterns of influence on EQI at each small regional scale, while rainfall impacts on EQI display a clear pattern at the provincial scale, following a decreasing trend from south to north (Figure 12). These findings suggest that the influence factors of vegetation growth differs with spatial location, and there are scale differences in the influence of factors on vegetation growth. Therefore, in our study, we used the MGWR model to examine the spatial heterogeneity of the influence of factors on EQI, and the Lindeman Merenda Gold (LMG) analysis was used to detect the relative importance of factors on EQI [48,49]. The LMG analysis results for Anhui Province from 2000 to 2018 indicated that elevation had the highest contribution to EQI, followed by human activities, slope, average temperature, and precipitation (Table 5). Comparing these results with the MGWR analysis, we found that they remained consistent, further confirming the reliability of our study.

**Table 5.** Relative importance of each factor on EQI.

Year	H	T	P	E	S
2000	15.09%	20.47%	13.54%	24.63%	26.26%
2005	17.96%	7.89%	16.56%	31.50%	26.09%
2010	23.48%	10.23%	14.47%	29.92%	21.90%
2015	30.72%	19.61%	9.56%	20.84%	19.28%
2018	24.49%	26.92%	10.04%	19.34%	19.21%
Mean	22.35%	17.02%	12.83%	25.25%	22.55%

## 6. Conclusions

The current study examines the spatiotemporal changes in vegetation ecological quality during the growth season in Anhui Province from 2000 to 2020. Utilizing a geographic weighted regression model, we explore the spatial heterogeneity of climate, terrain, and human activities on EQI. We draw the following conclusions.

Between 2000 and 2020, the vegetation ecological quality during the growth season in Anhui Province has significantly improved. The overall EQI reveals an upward trend, with an annual growth rate of 0.61%. Significantly increasing areas accounted for 43.49%, while significantly decreasing areas accounted for 3.60%.

EQI is positively correlated with precipitation ( $p < 0.1$ ) and negatively correlated with average temperature. Precipitation exhibits a greater impact, with rising altitudes and slopes leading to an increase followed by a decrease in EQI. Elevated human activity levels result in a deterioration of EQI with a significant negative correlation ( $p < 0.01$ ). The spatial dependence between human activities and EQI is mainly of the “high-low” type, where high EQI values are surrounded by low human activity areas.

EQI displayed significant spatial heterogeneity in its responsiveness to climate, topography, and human activities. The impact of human activities and topography on EQI was stronger at the local level, whereas climatic factors tended to exert a greater influence on EQI at the global level. In terms of magnitude, elevation had the strongest effect on EQI, followed by human activities, slope, average temperature, and precipitation.

**Author Contributions:** Writing—original draft, T.W.; writing—review and editing, M.Z. and T.W.; data curation, Y.G.; investigation, Z.Y.; supervision, Z.Z. All authors have read and agreed to the published version of the manuscript.

**Funding:** This project was funded by Anhui Provincial Natural Science Foundation, grant number 2208085MD88; National Natural Science Foundation of China, grant number 41501226; Research Fund for Doctoral Program of Anhui University of Science and Technology, grant number ZY020.

**Institutional Review Board Statement:** Not applicable.

**Informed Consent Statement:** Not applicable.

**Data Availability Statement:** Not applicable.

**Conflicts of Interest:** The authors declare no conflict of interest.

## References

1. Qian, S.; Cui, X.J.; Jiang, Y. QX/T 494-2019 Interpretation of QX/T 494-2019, Grade of monitoring and evaluating for terrestrial vegetation meteorology and ecological quality. *Std. Sci.* **2022**, *7*, 91–97+110. (In Chinese)
2. DeFries, R. Terrestrial Vegetation in the Coupled Human-Earth System: Contributions of Remote Sensing. *Annu. Rev. Environ. Resour.* **2008**, *33*, 369–390. [[CrossRef](#)]
3. Qiu, Z.; Feng, Z.; Song, Y.; Li, M.; Zhang, P. Carbon sequestration potential of forest vegetation in China from 2003 to 2050: Predicting forest vegetation growth based on climate and the environment. *J. Clean. Prod.* **2020**, *252*, 119715. [[CrossRef](#)]
4. Wei, X.; Wang, S.; Wang, Y. Spatial and temporal change of fractional vegetation cover in North-western China from 2000 to 2010. *Geol. J.* **2018**, *53*, 427–434. [[CrossRef](#)]
5. Song, L.; Li, Y.; Ren, Y.; Wu, X.; Guo, B.; Tang, X.; Shi, W.; Ma, M.; Han, X.; Zhao, L. Divergent vegetation responses to extreme spring and summer droughts in Southwestern China. *Agric. For. Meteorol.* **2019**, *279*, 107703. [[CrossRef](#)]

6. Li, Y.; Wu, D.; Yang, L.; Zhou, T. Declining Effect of Precipitation on the Normalized Difference Vegetation Index of Grasslands in the Inner Mongolian Plateau, 1982–2010. *Appl. Sci.* **2021**, *11*, 8766. [CrossRef]
7. Fu, D.J.; Xiao, H.; Su, F.Z.; Zhou, C.H.; Dong, J.W.; Zeng, Y.L.; Yan, K.; Li, S.W.; Wu, J.; Wu, W.Z.; et al. Remote sensing cloud computing platform development and Earth science application. *Nat. Remote Sens. Bull.* **2021**, *25*, 220–230. (In Chinese)
8. Gomes, V.C.F.; Queiroz, G.R.; Ferreira, K.R. An Overview of Platforms for Big Earth Observation Data Management and Analysis. *Remote Sens.* **2020**, *12*, 1253. [CrossRef]
9. Moore, R.; Hansen, M. Google Earth Engine: A New Cloud-Computing Platform for Global-Scale Earth Observation Data and Analysis. In Proceedings of the American Geophysical Union Fall Meeting 2011, San Francisco, CA, USA, 5–9 December 2011.
10. Tamiminia, H.; Salehi, B.; Mahdianpari, M.; Quackenbush, L.; Adeli, S.; Brisco, B. Google Earth Engine for geo-big data applications: A meta-analysis and systematic review. *ISPRS J. Photogramm. Remote Sens.* **2020**, *164*, 152–170. [CrossRef]
11. Amani, M.; Ghorbanian, A.; Ahmadi, S.A.; Kakooei, M.; Moghimi, A.; Mirmazloumi, S.M.; Moghaddam, S.H.A.; Mahdavi, S.; Ghahremanloo, M.; Parsian, S.; et al. Google Earth Engine Cloud Computing Platform for Remote Sensing Big Data Applications: A Comprehensive Review. *IEEE J. Sel. Top. Appl. Earth Observ. Remote Sens.* **2020**, *13*, 5326–5350. [CrossRef]
12. Chuai, X.W.; Huang, X.J.; Wang, W.J.; Bao, G. NDVI, temperature and precipitation changes and their relationships with different vegetation types during 1998–2007 in Inner Mongolia, China. *Int. J. Clim.* **2013**, *33*, 1696–1706. [CrossRef]
13. Liu, H.; Zheng, L.; Yin, S. Multi-perspective analysis of vegetation cover changes and driving factors of long time series based on climate and terrain data in Hanjiang River Basin, China. *Arab. J. Geosci.* **2018**, *11*, 509. [CrossRef]
14. Xiao, J.; Zhou, Y.; Zhang, L. Contributions of natural and human factors to increases in vegetation productivity in China. *Ecosphere* **2015**, *6*, 233. [CrossRef]
15. Luo, L.; Ma, W.; Zhuang, Y.; Zhang, Y.; Yi, S.; Xu, J.; Long, Y.; Ma, D.; Zhang, Z. The impacts of climate change and human activities on alpine vegetation and permafrost in the Qinghai-Tibet Engineering Corridor. *Ecol. Indic.* **2018**, *93*, 24–35. [CrossRef]
16. Cheng, D.; Qi, G.; Song, J.; Zhang, Y.; Bai, H.; Gao, X. Quantitative Assessment of the Contributions of Climate Change and Human Activities to Vegetation Variation in the Qinling Mountains. *Front. Earth Sci.* **2021**, *9*, 782287. [CrossRef]
17. Luo, H.X.; Dai, S.P.; Li, M.F.; Li, Y.P.; Zheng, Q.; Hu, Y.Y. Relative roles of climate changes and human activities in vegetation variables in Hainan Island. *Remote Sens. Nat. Resour.* **2020**, *32*, 154–161. (In Chinese)
18. Zhang, L.Y.; Li, X.; Feng, J.H.; Rao, Y.G.; He, T.Y.; Chen, Y. Spatial-temporal Changes of NDVI in Yellow River Basin and Its Dual Response to Climate Change and Human Activities During 2000–2018. *Bull. Soil Water Conserv.* **2021**, *41*, 276–286. (In Chinese) [CrossRef]
19. Sanderson, E.W.; Jaiteh, M.; Levy, M.A.; Redford, K.H.; Wannebo, A.V.; Woolmer, G. The Human Footprint and the Last of the Wild: The Human Footprint Is a Global Map of Human Influence on the Land Surface, Which Suggests That Human Beings Are Stewards of Nature, Whether We like It or Not. *BioScience* **2002**, *52*, 891–904. [CrossRef]
20. Venter, O.; Sanderson, E.W.; Magrath, A.; Allan, J.R.; Beher, J.; Jones, K.R.; Possingham, H.P.; Laurance, W.F.; Wood, P.; Fekete, B.M.; et al. Sixteen years of change in the global terrestrial human footprint and implications for biodiversity conservation. *Nat. Commun.* **2016**, *7*, 12558. [CrossRef]
21. Mu, H.; Li, X.; Wen, Y.; Huang, J.; Du, P.; Su, W.; Miao, S.; Geng, M. A global record of annual terrestrial Human Footprint dataset from 2000 to 2018. *Sci. Data* **2022**, *9*, 176. [CrossRef]
22. Venter, O.; Sanderson, E.W.; Magrath, A.; Allan, J.R.; Beher, J.; Jones, K.R.; Possingham, H.P.; Laurance, W.F.; Wood, P.; Fekete, B.M.; et al. Global terrestrial Human Footprint maps for 1993 and 2009. *Sci. Data* **2016**, *3*, 160067. [CrossRef] [PubMed]
23. Wu, T.; Zhou, L.; Jiang, G.; Meadows, M.E.; Zhang, J.; Pu, L.; Wu, C.; Xie, X. Modelling Spatial Heterogeneity in the Effects of Natural and Socioeconomic Factors, and Their Interactions, on Atmospheric PM<sub>2.5</sub> Concentrations in China from 2000–2015. *Remote Sens.* **2021**, *13*, 2152. [CrossRef]
24. Yue, H.; Duan, L.; Lu, M.; Huang, H.; Zhang, X.; Liu, H. Modeling the Determinants of PM<sub>2.5</sub> in China Considering the Localized Spatiotemporal Effects: A Multiscale Geographically Weighted Regression Method. *Atmosphere* **2022**, *13*, 627. [CrossRef]
25. Zhang, J.; Liu, X.; Tan, X.; Jia, T.; Senousi, A.M.; Huang, J.; Yin, L.; Zhang, F. Nighttime Vitality and Its Relationship to Urban Diversity: An Exploratory Analysis in Shenzhen, China. *IEEE J. Sel. Top. Appl. Earth Obs. Remote Sens.* **2022**, *15*, 309–322. [CrossRef]
26. Zhou, M.; Li, Y.; Zhang, F. Spatiotemporal Variation in Ground Level Ozone and Its Driving Factors: A Comparative Study of Coastal and Inland Cities in Eastern China. *Int. J. Environ. Res. Public Health* **2022**, *19*, 9687. [CrossRef] [PubMed]
27. Grade of Monitoring and Evaluating for Terrestrial Vegetation Meteorology and Ecological Quality. Available online: [https://www.cma.gov.cn/zfxgk/gknr/flfgbz/bz/202209/t20220921\\_5099232.html](https://www.cma.gov.cn/zfxgk/gknr/flfgbz/bz/202209/t20220921_5099232.html) (accessed on 22 December 2022).
28. De Jager, N.R.; Fox, T.J. Curve Fit: A pixel-level raster regression tool for mapping spatial patterns. *Methods Ecol. Evol.* **2013**, *4*, 789–792. [CrossRef]
29. Xu, Y.; Huang, W.-T.; Dou, S.-Q.; Guo, Z.-D.; Li, X.-Y.; Zheng, Z.-W.; Jing, J.-L. Responding Mechanism of Vegetation Cover to Climate Change and Human Activities in Southwest China from 2000 to 2020. *Huanjing KeXue* **2022**, *43*, 3230–3240. [CrossRef]
30. Shi, S.; Wang, P.; Zhang, Y.; Yu, J. Cumulative and time-lag effects of the main climate factors on natural vegetation across Siberia. *Ecol. Indic.* **2021**, *133*, 108446. [CrossRef]
31. Yao, S.W.; Zeng, J.; Li, W.J. Spatial correlation characteristics of urbanization and land ecosystem service value in Wuhan Urban Agglomeration. *Trans. Chin. Soc. Agric. Eng.* **2015**, *31*, 249–256. (In Chinese)
32. Anselin, L. The Local Indicators of Spatial Association—LISA. *Geogr. Anal.* **1995**, *27*, 93–115. [CrossRef]

33. Ord, J.K.; Getis, A. Local Spatial Autocorrelation Statistics: Distributional Issues and an Application. *Geogr. Anal.* **1995**, *27*, 286–306. [[CrossRef](#)]
34. Anselin, L.; Rey, S.J. *Modern Spatial Econometrics in Practice: A Guide to Geoda, Geodaspace and PySAL*; GeoDa Press LLC: Chicago, IL, USA, 2014.
35. Zhou, T.; Chen, W.X.; Li, J.F.; Liang, J.L. Spatial relationship between human activities and habitat quality in Shennongjia Forest Region from 1995 to 2015. *Acta Ecol. Sin.* **2021**, *41*, 6134–6145. (In Chinese)
36. Oshan, T.M.; Li, Z.; Kang, W.; Wolf, L.J.; Fotheringham, A.S. Mgw: A Python Implementation of Multiscale Geographically Weighted Regression for Investigating Process Spatial Heterogeneity and Scale. *ISPRS Int. J. Geo Inf.* **2019**, *8*, 269. [[CrossRef](#)]
37. Shen, T.Y.; Yu, H.C.; Zhou, L.; Gu, H.Y.; He, H.H. On Hedonic Price of Second-Hand Houses in Beijing Based on Multi-Scale Geographically Weighted Regression: Scale Law of Spatial Heterogeneity. *Econ. Geogr.* **2020**, *40*, 75–83. (In Chinese) [[CrossRef](#)]
38. Gu, Z.N.; Zhang, Z.; Hu, K.Q.; Lu, Y.J. Analysis on the Normalized Difference Vegetation Index Change and Influence Factors in Anhui Province Based on Structural Equation Model. *Sci. Technol. Eng.* **2022**, *22*, 12259–12267. (In Chinese)
39. Wang, Y.; Liao, J.; Ye, Y.; Fan, J. Long-term human expansion and the environmental impacts on the coastal zone of China. *Front. Mar. Sci.* **2022**, *9*, 5279. [[CrossRef](#)]
40. Zhao, Z.; Li, T.; Zhang, Y.; Lü, D.; Wang, C.; Lü, Y.; Wu, X. Spatiotemporal Patterns and Driving Factors of Ecological Vulnerability on the Qinghai-Tibet Plateau Based on the Google Earth Engine. *Remote Sens.* **2022**, *14*, 5279. [[CrossRef](#)]
41. Meng, Z.; Dong, J.; Ellis, E.C.; Metternicht, G.; Qin, Y.; Song, X.-P.; Löfqvist, S.; Garrett, R.D.; Jia, X.; Xiao, X. Post-2020 biodiversity framework challenged by cropland expansion in protected areas. *Nat. Sustain.* **2023**, *6*, 1–11. [[CrossRef](#)]
42. Bai, Y.; Jiang, B.; Wang, M.; Li, H.; Alatalo, J.M.; Huang, S. New ecological redline policy (ERP) to secure ecosystem services in China. *Land Use Policy* **2016**, *55*, 348–351. [[CrossRef](#)]
43. Zhang, K.; Wen, Z. Review and challenges of policies of environmental protection and sustainable development in China. *J. Environ. Manag.* **2008**, *88*, 1249–1261. [[CrossRef](#)]
44. Li, L.; Fan, Z.; Xiong, K.; Shen, H.; Guo, Q.; Dan, W.; Li, R. Current situation and prospects of the studies of ecological industries and ecological products in eco-fragile areas. *Environ. Res.* **2021**, *201*, 111613. [[CrossRef](#)] [[PubMed](#)]
45. Gong, Z.; Zhao, S.; Gu, J. Correlation analysis between vegetation coverage and climate drought conditions in North China during 2001–2013. *J. Geogr. Sci.* **2017**, *27*, 143–160. [[CrossRef](#)]
46. Lasaponara, R. On the use of principal component analysis (PCA) for evaluating interannual vegetation anomalies from SPOT/VEGETATION NDVI temporal series. *Ecol. Model.* **2006**, *194*, 429–434. [[CrossRef](#)]
47. Li, M.; Yan, Q.; Li, G.; Yi, M.; Li, J. Spatio-Temporal Changes of Vegetation Cover and Its Influencing Factors in Northeast China from 2000 to 2021. *Remote Sens.* **2022**, *14*, 5720. [[CrossRef](#)]
48. Grömping, U. Estimators of Relative Importance in Linear Regression Based on Variance Decomposition. *Am. Stat.* **2007**, *61*, 139–147. [[CrossRef](#)]
49. Shi, P.; Chen, Y.; Zhang, G.; Tang, H.; Chen, Z.; Yu, D.; Yang, J.; Ye, T.; Wang, J.; Liang, S.; et al. Factors contributing to spatial-temporal variations of observed oxygen concentration over the Qinghai-Tibetan Plateau. *Sci. Rep.* **2021**, *11*, 17338. [[CrossRef](#)]

**Disclaimer/Publisher’s Note:** The statements, opinions and data contained in all publications are solely those of the individual author(s) and contributor(s) and not of MDPI and/or the editor(s). MDPI and/or the editor(s) disclaim responsibility for any injury to people or property resulting from any ideas, methods, instructions or products referred to in the content.